

The Data Forecast in COVID-19 Model with Applications to US, South Korea, Brazil, India, Russia and Italy

Bo-Cyuan Lin*, Yen-Jia Chen[†], Yi-Cheng Hung[†], Chun-sheng Chen*, Han-Chun Wang*, Jann-Long Chern[‡]

*Department of Mathematics, National Central University, Taoyuan, Taiwan. [†]Department of Mathematics, National Taiwan Normal University, Taipei, Taiwan. [‡]Corresponding author. Department of Mathematics, National Central University, Taoyuan, Taiwan. The authors are supported in part by Ministry of Science and Technology (MOST), Taiwan, No. MOST 107-2115-M008-005-MY3, and 2020 NCTS USRP, Taiwan.

Abstract—In this paper, we firstly propose SQIARD and SIARD models to investigate the transmission of COVID-19 with quarantine, infected and asymptomatic infected, and discuss the relation between the respective basic reproduction number R_0 , R_Q and the stability of the equilibrium points of model. Secondly, after training the related data parameters, in our numerical simulations, we respectively conduct the forecast of the data of US, South Korea, Brazil, India, Russia and Italy, and the effect of prediction of the epidemic situation in each country. Furthermore, we apply US data to compare SQIARD with SIARD, and display the effects of predictions.

Index Terms—COVID-19, quarantine, asymptomatic infection, SIARD Model, SQIARD Model, data forecast

I. INTRODUCTION

Since the first Coronavirus disease (COVID-19) patient was discovered in Wuhan, China in December 2019, it has become the most serious infectious disease in the world today. According to the reports of “WHO Coronavirus Disease (COVID-19) Dashboard”, globally, as of 3:02pm CEST, 24 October 2020, there have been 42,055,863 confirmed cases of COVID-19, including 1,141,567 deaths. This disease poses a great threat to the health of the global population and damages various developments in the world.

There is a lot of evidence that COVID-19 patients have a very high proportion of patients with mild symptoms or no symptoms. As a support to the possibility that there are less symptomatic cases than previously estimated. In [1], the authors estimated that in 11 European countries, there are orders of magnitude fewer infections detected than true infections, mostly likely due to mild and asymptomatic infections as well as limited testing capacity. Lavezzo, et al [2] stated that, at Vò, Italy, the asymptomatic cases were a fraction of 43.2% of the total. In [3], the article assumed that the asymptomatic infected population is about nine times larger than the population with symptoms, based on government estimations. Gudbjartsson, et al [4] also pointed out that in the overall population screening group in Iceland, SARS-CoV-2 43% of the participants who tested positive were asymptomatic. In [5], it found that the proportion of asymptomatic individuals increased very fast from 16.1%(35 asymptomatic infections/218 confirmed cases) to 50.6%(314/621) a week. From this researching results, we observed that the proportion of asymptomatic infections for

COVID-19 has dramatic changed. By the WHO’s report, it also pointed out that the asymptomatic infections are not non-infectious more and more. Therefore, the proportion of asymptomatic infections is critical to the impact of epidemic research. In this paper, we will use mathematical models and data analysis methods to analyze the proportion of asymptomatic infections in various countries and predict the future trend of the epidemic. In Table 1 of section 4, we list the proportion of symptomatic infections α in six countries, respectively. $1-\alpha$ is the proportion of asymptomatic people. In [2], the authors also stated that, at Vò, Italy, the asymptomatic cases were a fraction of 43.2 % of the total, which was consistent with the 45 % of our numerical simulation in the Table 1 for Italy. This also shows that our model can be applied to find out the proportion of asymptomatic people in each country.

In the study of the COVID-19 epidemic, one of important topics is to estimate the basic reproduction number R_0 . In [7] and [8], they found the relation between the model locally asymptotically stability and R_0 . In [9], the authors found out the relation between the globally asymptotically stability of the model and R_0 . In the nice results of [10], Chen, et al revised the respective model into discrete time difference equations to find the representation of each parameter. Then they further used the iterative method to find the relation between R_0 and model parameters. In our article, we will first use the stability of the model itself to find out the relation between R_0 and model parameters, and further revise our differential systems into discrete time difference equations to train the model parameters for the epidemic prediction respectively.

In the previous SARS epidemic, many researchers have discussed the modifications of the SARS epidemic in terms of “quarantine” and “asymptomatic”, e.g., please refer to [7]-[8] and the related references. However, because SARS and COVID-19 have different epidemic patterns, the disease patterns of asymptomatic infections are also different. Therefore, we establish two mathematical models, SQIARD and SIARD model, to simulate the COVID-19 epidemic. Strictly speaking, the SIARD model is only a simplified form of the SQIARD model. The difference between the two models is whether the parameters “number of people to be screened for the epidemic” is added. As the acquisition of this parameter is very difficult,

currently the United States has complete data on the number of people in quarantine that can be used to train the model parameters. In order to train the related model parameters, we remove the parameter $Q(t)$ and use the SIARD model to conduct the prediction data of US, South Korea, Brazil, India, Russia and Italy. We will first propose the effect of prediction of the SIARD model, and then use US data which contains $Q(t)$ to show the effect of prediction of the SQIARD model.

The article is organized as follows: In Section 2, we propose SQIARD to investigate the transmission of COVID-19 with quarantine, infected and asymptomatic infected, and discuss the relation between stability of the equilibrium points and R_Q . In our numerical simulation, we will observe that SQIARD is available to conduct the forecast in US. In Section 3, we establish the SIARD model, also use FIR to train its parameters and discuss R_0 with the stability of equilibrium for the model. Finally, in Section 4, we will show and discuss the forecast of the data of US, South Korea, Brazil, India, Russia and Italy, and the effect of prediction of the epidemic situation in each country. At the same time, we use US data to compare SQIARD with SIARD, and display the effects of predictions.

II. SQIARD MODEL

In this section, for consideration of the high proportion of patients with mild symptoms or no symptoms and the people with possibility of negative for the coronavirus back to the susceptible group after the quarantine, we propose our model, SQIARD to investigate the transmission of COVID-19 with quarantine, infected and asymptomatic infected. First, we give some assumptions for SQIARD and its relative basic reproduction number; Secondly, in our numerical simulation, we will observe that SQIARD is available to conduct the forecast in US; Thirdly, we discuss the relation between stability of the equilibrium points and R_Q .

A. The Derivation and Basic Reproduction Number

The model has the following assumptions:

- 1) $Q(t)$ is the number of quarantine people per day. Those with positive quarantine results are further divided into "symptomatic patients" ($I(t)$) or "asymptomatic patients" ($A(t)$). Those with negative quarantine results will return to $S(t)$ at a rate of μ_3 .
- 2) $A(t)$ is claimed to be had less infectivity, $0 < \delta < 1$, where δ is the proportion in infectiousness of asymptomatic infectives.
- 3) Total Population in our model are viewed as the same.
- 4) We simply the total population as a fixed value without new born and non-epidemic death.

The variables are given as follows: [S : susceptible population; Q : quarantine population; I : infective population; A : asymptomatic infective population; R : recovered population; D : deaths].

The model parameters are given as follows: [β : the progression rate of susceptible to quarantine classes; δ : the proportion in infectiousness of asymptomatic infectives, where $0 < \delta < 1$; μ_1 : the progression rate of susceptible to infective

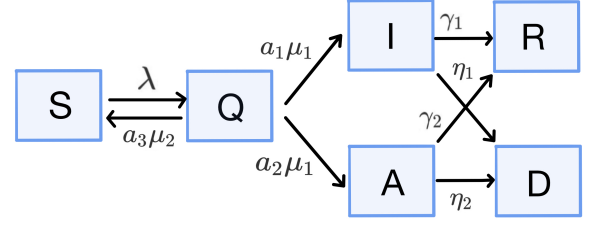


Fig. 1. The flow chart of SQIARD

classes; μ_2 : the progression rate of quarantine to susceptible classes; a_i : with $0 < a_i < 1$, the proportion of susceptible class Q progressing to positive class I , A , or negative class which will back to the susceptible S , and $a_1 + a_2 + a_3 = 1$; γ_1 and γ_2 : the recovered rates of infective classes I and A ; η_1 and η_2 : are the disease death rates of infective classes I and A].

From above, $S(t)$, $Q(t)$, $I(t)$, $A(t)$, $R(t)$ and $D(t)$ are conducted by the following differential equations:

$$\begin{cases} S' = -\lambda S + a_3\mu_2 Q \\ Q' = \lambda S - (a_1\mu_1 + a_2\mu_1 + a_3\mu_2) Q \\ I' = a_1\mu_1 Q - (\gamma_1 + \eta_1) I \\ A' = a_2\mu_1 Q - (\gamma_2 + \eta_2) A \\ R' = \gamma_1 I + \gamma_2 A \\ D' = \eta_1 I + \eta_2 A, \end{cases} \quad (1)$$

where $\lambda = \frac{\beta(I + \delta A)}{(S + I + A)}$, $S(0) = S_0 > 0$, $Q(0) = 0$, $I(0) = I_0 > 0$, $A(0) = A_0 > 0$, $R(0) = 0$ and $D(0) = 0$. We note that $S(t) + Q(t) + I(t) + A(t) + R(t) + D(t) = N = S_0 + I_0 + A_0$ where N is the total population.

The basic reproduction number of (1) is:

$$R_Q = \frac{\mu_1}{a_1\mu_1 + a_2\mu_1 + a_3\mu_2} \left[\frac{a_1}{\gamma_1 + \eta_1} + \frac{a_2\delta}{\gamma_2 + \eta_2} \right] \beta. \quad (2)$$

Due to daily updating of the COVID-19, we revise (1) into discrete form (3) and (4):

$$\begin{aligned} S(t+1) - S(t) &= -\frac{\beta S(I + \delta A)}{S + I + A} + a_3\mu_2 Q(t) \\ R(t+1) - R(t) &= \gamma_1 I + \gamma_2 A \\ D(t+1) - D(t) &= \eta_1 I + \eta_2 A. \end{aligned} \quad (3)$$

When the disease first spreads, the number of people infected is much smaller than the total population. The total population can be assumed to be the same as the number of suspected infections and let $q = (a_1\mu_1 + a_2\mu_1 + a_3\mu_2)$ further

simplify as follows :

$$I(t+1) - I(t) = a_1\mu_1 Q(t) - \gamma_1 I - \eta_1 I$$

$$A(t+1) - A(t) = a_2\mu_1 Q(t) - \gamma_2 A - \eta_2 A \quad (4)$$

$$Q(t+1) - Q(t) = \beta(I + \delta A) - qQ(t).$$

Write above formula in the matrix form yields the following equation:

$$\begin{bmatrix} I(t+1) \\ A(t+1) \\ Q(t+1) \end{bmatrix} = \begin{bmatrix} 1 - (\gamma_1 + \eta_1) & 0 & a_1\mu_1 \\ 0 & 1 - (\gamma_2 + \eta_2) & a_2\mu_1 \\ \beta & \beta\delta & 1 - q \end{bmatrix} \begin{bmatrix} I(t) \\ A(t) \\ Q(t) \end{bmatrix}.$$

Let M be the transmission matrix of the system equations. Then

$$M = \begin{bmatrix} 1 - (\gamma_1 + \eta_1) & 0 & a_1\mu_1 \\ 0 & 1 - (\gamma_2 + \eta_2) & a_2\mu_1 \\ \beta & \beta\delta & 1 - q \end{bmatrix}.$$

It is well know that such a system is stable if the spectral radius of M is less than 1. In this case, $I(t+1)$, $A(t+1)$ and $Q(t+1)$ will converge asymptotically to a respectively finite constant as $t \rightarrow \infty$. In the following theorem, we show that there is no outbreak if $R_Q < 1$ and outbreak if $R_Q > 1$. Thus, R_Q is known as the threshold for an outbreak in such a model.

Theorem II.1. The following statements are equivalent :

- (a) $M - I$ is stable
- (b) $R_Q < 1$
- (c) $\rho(M) < 1$

Proof: (a) \Leftrightarrow (b) :

Let

$$M - I = \begin{bmatrix} -(\gamma_1 + \eta_1) & 0 & a_1\mu_1 \\ 0 & -(\gamma_2 + \eta_2) & a_2\mu_1 \\ \beta & \beta\delta & -q \end{bmatrix}.$$

Then the characteristic polynomial of $M - I$ is

$$\begin{aligned} f(\lambda) &= \lambda^3 + (D_1 + D_2 + q)\lambda^2 + D_1D_2 + (D_1 + D_2)q \\ &\quad - \beta a_1\mu_1 - \beta\delta a_2\mu_1\lambda + D_1D_2q \\ &\quad - \beta a_1\mu_1D_2 - \beta\delta a_2\mu_1D_1 \\ &\equiv c_1\lambda^3 + c_2\lambda^2 + c_3\lambda + c_4, \end{aligned}$$

where $D_1 = (\gamma_1 + \eta_1)$, $D_2 = (\gamma_2 + \eta_2)$.

If all eigenvalues of $M - I$ have negative real parts, then $M - I$ is stable, and, by **Routh-Hurwitz criterion**, we obtain the follows:

$$\begin{cases} c_1 = 1 > 0 \\ c_2 = (D_1 + D_2 + q) > 0 \\ c_3 = [D_1D_2 + (D_1 + D_2)q - \beta a_1\mu_1 - \beta\delta a_2\mu_1] > 0 \\ c_4 = D_1D_2q - \beta a_1\mu_1D_2 - \beta\delta a_2\mu_1D_1 > 0 \\ c_2c_3 > c_1c_4 \end{cases}$$

We can get the following inequality through simple calculations,

$$\begin{aligned} \beta &< \min\left\{\frac{D_1D_2 - (D_1 + D_2)q}{\mu_1(a_1 + a_2\delta)}, \frac{D_1D_2q}{\mu_1(a_1D_2 + a_2\delta D_1)}, \right. \\ &\quad \left. \frac{(D_1 + D_2)[D_1D_2 + q(D_1 + D_2 + q)]}{\mu_1[a_1(q + D_1) + a_2\delta(q + D_2)]}\right\} \\ &= \frac{D_1D_2q}{\mu_1(a_1D_2 + a_2\delta D_1)}. \end{aligned}$$

It's easy to show that $\beta < \frac{D_1D_2q}{\mu_1(a_1D_2 + a_2\delta D_1)}$ if and only if

$$R_Q = \frac{\mu_1}{q} \left(\frac{a_1}{D_1} + \frac{a_2\delta}{D_2} \right) \beta < 1.$$

This shows (a) \Leftrightarrow (b).

Now, we want to show the proof of (a) \Leftrightarrow (c). First, we prove (a) \rightarrow (c). Let $M - I$ be stable. We consider the following two case :

- 1) $\sigma(M - I) \subseteq \mathbb{R}$

We may assume $\lambda_i \in \sigma(M - I)$ and $\lambda_3 \leq \lambda_2 \leq \lambda_1 < 0$. Then it implies $\lambda_i + 1 \in \sigma(M)$. $\forall i..$ Since M is a positive matrix, by **Perron-Frobenius Theorem**, we have $\rho(M) \in \sigma(M)$ and $\rho(M) > 0$.

Hence, it's easy to see that $\rho(M) = \lambda_1 + 1 \in (0, 1)$.

Then we obtain $\rho(M) < 1$.

- 2) $\sigma(M - I) = \{\lambda, a \pm bi | \lambda, a, b \in \mathbb{R}\}$

We may assume that λ and a are negative.

Since M is a positive matrix, by **Perron-Frobenius Theorem**, we have $\rho(M) \in \sigma(M)$ and $\rho(M) > 0$. Assume that $\rho(M) \neq \lambda + 1 \in (0, 1)$, it implies $\rho(M) < 1$.

Now, we prove (c) \rightarrow (a) in the following.

Let $\rho(M) < 1$, i.e. $\lambda_i \in \sigma(M)$ and $|\lambda_i| < 1$. for $i = 1, 2$.

- a) $\lambda_i \in \mathbb{R}, \forall i$, then $\lambda_i - 1 \in \sigma(M - I)$ and $\lambda_i - 1 < 0$ for $i = 1, 2, 3$.
- b) If $\lambda_1 \in \mathbb{R}, \lambda_2 = a + bi$ and $\lambda_3 = a - bi$, then $|\lambda_2| = |\lambda_3| = a^2 + b^2 < 1$ and $|\lambda_1| < 1$. It follows that $|a| < 1$.

Since $\sigma(M - I) = \{\lambda_1 - 1, (a - 1) \pm bi\}$, then

- a) $\lambda < 1 \Rightarrow \lambda - 1 < 0$,
- b) $|a| < 1 \Rightarrow a - 1 \in (-2, 0) \Rightarrow \text{Re}(\lambda_2) = \text{Re}(\lambda_3) < 0$.

Therefore, $M - I$ is stable.

This completes the proof of Theorem II.1. ■

The following Corollary states the relation of R_Q and the breaking property of the epidemic.

Corollary II.1. If $R_Q < 1$ then there is no outbreak of the epidemic. Moreover, if $R_Q > 1$, then there is an outbreak of epidemic.

Proof: Let $X(t) = \begin{bmatrix} I(t) \\ A(t) \\ Q(t) \end{bmatrix}$. According to the previous assumptions, we can get $\dot{X} = (\mathbf{M} - \mathbf{I})X$ and $X(0) = X_0$. Hence, we have $X = Pe^{Dt}P^{-1}X_0$ where $P^{-1}(\mathbf{M} - \mathbf{I})P = D = \begin{bmatrix} \lambda_1 - 1 & 0 & 0 \\ 0 & \lambda_2 - 1 & 0 \\ 0 & 0 & \lambda_3 - 1 \end{bmatrix}$, and $\lambda_1 \geq \lambda_2 \geq \lambda_3$. By Theorem II.1, the followings are true:

- 1) If $\rho(\mathbf{M}) < 1$, $\lambda_i - 1 \leq \rho(\mathbf{M}) - 1 < 0$ for $i = 1, 2, 3$, then $X(t)$ converge to $\mathbf{0}$ as $t \rightarrow \infty$.
- 2) If $\rho(\mathbf{M}) > 1$, $\lambda_1 - 1 = \rho(\mathbf{M}) - 1 > 0$, then $\|X(t)\| \rightarrow \infty$ as $t \rightarrow \infty$.

This completes the proof. \blacksquare

B. Tracking Time-Depend SQUIARD Model Algorithms

To predict the Covid-19 data which is discrete with time series, we consider the differential equations in section 2.1 as discrete form:

$$\begin{cases} S(t+1) = S(t) - \frac{\beta(t)S(t)(I(t) + \delta A(t))}{S(t) + I(t) + A(t)} + a_3(t)\mu_2 Q(t) \\ Q(t+1) = Q(t) + \frac{\beta(t)S(t)(I(t) + \delta A(t))}{S(t) + I(t) + A(t)} \\ \quad - (a_1(t)\mu_1 + a_2(t)\mu_1 + a_3(t)\mu_2)Q(t) \\ I(t+1) = I(t) + a_1(t)\mu_1 Q(t) - \gamma_1(t)I(t) - \eta_1(t)I(t) \\ A(t+1) = A(t) + a_2(t)\mu_1 Q(t) - \gamma_2(t)A(t) - \eta_2(t)A(t) \\ R(t+1) = R(t) + \gamma_1(t)I(t) + \gamma_2(t)A(t) \\ D(t+1) = D(t) + \eta_1(t)I(t) + \eta_2(t)A(t) \end{cases} \quad (5)$$

If the asymptomatic infected people die in a very low probability, then we can consider $\eta_2 = 0$. Then, in this case, since the relation $a_1 + a_2 + a_3 = 1$, the $\beta(t)$, $\gamma_1(t)$, $\gamma_2(t)$, $\eta_1(t)$, $a_3(t)$ and the time-depend basic reproduction number of SQUIARD can be evolved as following (6) and (7):

$$\begin{aligned} \beta(t) &= \frac{(S(t) - S(t+1) + a_3\mu_2 Q(t))}{S(t)(I(t) + \delta A(t))} (S(t) + I(t) + A(t)) \\ \gamma_1(t) &= \frac{I(t) - I(t+1) + a_1\mu_1 Q(t)}{I(t)} \\ \gamma_2(t) &= \frac{R(t+1) - R(t) + I(t+1) - I(t) + a_1\mu_1 Q(t)}{A(t)} \\ \eta_1(t) &= \frac{D(t+1) - D(t)}{I(t)} \\ a_3(t) &= \frac{S(t+1) - S(t) + Q(t+1) - Q(t) + \mu_1 Q(t)}{\mu_1 Q(t)} \end{aligned} \quad (6)$$

$$R_Q(t) = \frac{\beta(t)\mu_1}{(a_1(t)\mu_1 + a_2(t)\mu_1 + a_3(t)\mu_2)} \left(\frac{a_1(t)}{\gamma_1(t) + \eta_1(t)} + \frac{\delta a_2(t)}{\gamma_2(t)} \right). \quad (7)$$

Since the data of Covid-19 contains $\{S(t), Q(t), I(t), R(t), D(t), 0 \leq t \leq T\}$, we consider $A(t) = \alpha * I(t)$,

$I(t) = (1 - \alpha) * I(t)$, and $\delta = 0.5$ (the infection rate of asymptom about 0.5). Then, after calculating the data $\{\beta(t), \gamma_1(t), \gamma_2(t), \eta_1(t), a_3(t), 0 \leq t \leq T-1\}$, we can use the machine learning method, e.g., the following methods of Finite Impulse Response filters (FIR), to predict $\hat{\beta}(t), \hat{\gamma}_1(t), \hat{\gamma}_2(t), \hat{\eta}_1(t), \hat{a}_3(t)$. We note that $\hat{a}_1(t), \hat{a}_2(t)$ can be obtained from $\hat{a}_3(t)$.

$$\begin{aligned} \hat{\beta}(t) &= a_0 + a_1\beta(t-1) + \dots + a_{J_1}\beta(t-J_1) \\ &= \sum_{j=1}^{J_1} a_j\beta(t-j) + a_0 \\ \hat{\gamma}_1(t) &= b_0 + b_1\gamma_1(t-1) + \dots + b_{J_2}\gamma_1(t-J_2) \\ &= \sum_{j=1}^{J_2} b_j\gamma_1(t-j) + b_0 \\ \hat{\gamma}_2(t) &= c_0 + c_1\gamma_2(t-1) + \dots + c_{J_3}\gamma_2(t-J_3) \\ &= \sum_{j=1}^{J_3} c_j\gamma_2(t-j) + c_0 \\ \hat{\eta}_1(t) &= d_0 + d_1\eta_1(t-1) + \dots + d_{J_4}\eta_1(t-J_4) \\ &= \sum_{j=1}^{J_4} d_j\eta_1(t-j) + d_0 \\ \hat{a}_3(t) &= e_0 + e_1a_3(t-1) + \dots + e_{J_5}a_3(t-J_5) \\ &= \sum_{j=1}^{J_5} e_ja_3(t-j) + e_0, \end{aligned} \quad (8)$$

where $a_{j_1}, j_1 = 0, 1, \dots, J_1$; $b_{j_2}, j_2 = 0, 1, \dots, J_2$; $c_{j_3}, j_3 = 0, 1, \dots, J_3$; $d_{j_4}, j_4 = 0, 1, \dots, J_4$; $e_{j_5}, j_5 = 0, 1, \dots, J_5$ are the coefficients (weight) of the five given FIR filters as above.

We will adopt the following Ridge Regularization method (9), which is often used in the machine learning for each FIR models, and use Theorem II.2 implemented by Algorithm 1 to optimize the respective weights:

$$\begin{aligned} \min_{\{\mathbf{a}\}} F_{\beta}(\mathbf{a}) &= \min_{\{\mathbf{a}\}} \left[\sum_{t=J_1}^{T-2} (\beta(t) - \hat{\beta}(t))^2 + m_1 \sum_{i=0}^{J_1} a_i^2 \right] \\ \min_{\{\mathbf{b}\}} F_{\gamma_1}(\mathbf{b}) &= \min_{\{\mathbf{b}\}} \left[\sum_{t=J_2}^{T-2} (\gamma_1(t) - \hat{\gamma}_1(t))^2 + m_2 \sum_{i=0}^{J_2} b_i^2 \right] \\ \min_{\{\mathbf{c}\}} F_{\gamma_2}(\mathbf{c}) &= \min_{\{\mathbf{c}\}} \left[\sum_{t=J_3}^{T-2} (\gamma_2(t) - \hat{\gamma}_2(t))^2 + m_3 \sum_{i=0}^{J_3} c_i^2 \right] \\ \min_{\{\mathbf{d}\}} F_{\eta_1}(\mathbf{d}) &= \min_{\{\mathbf{d}\}} \left[\sum_{t=J_4}^{T-2} (\eta_1(t) - \hat{\eta}_1(t))^2 + m_4 \sum_{i=0}^{J_4} d_i^2 \right] \\ \min_{\{\mathbf{e}\}} F_{a_3}(\mathbf{e}) &= \min_{\{\mathbf{e}\}} \left[\sum_{t=J_5}^{T-2} (a_3(t) - \hat{a}_3(t))^2 + m_5 \sum_{i=0}^{J_5} e_i^2 \right] \end{aligned} \quad (9)$$

, where $\mathbf{a} = (a_0, a_1, \dots, a_{J_1})$, $\mathbf{b} = (b_0, b_1, \dots, b_{J_2})$, $\mathbf{c} = (c_0, c_1, \dots, c_{J_3})$, $\mathbf{d} = (d_0, d_1, \dots, d_{J_4})$, $\mathbf{e} = (e_0, e_1, \dots, e_{J_5})$.

1) Normal Gradient Equation:

Theorem II.2. (Normal Gradient Equation)

Let $f(0), f(1), \dots, f(T-2)$ be the training data with $T-1$ points, and the FIR filter $\hat{f}(t) = x_0 + x_1 f(t-1) + \dots + x_J f(t-J)$ be the prediction of t -th point, $t = J, \dots, T-2$ with cost function $F(x_0, x_1, \dots, x_J; m) = \sum_{t=J}^{T-2} (f(t) - \hat{f}(t))^2 + m \sum_{i=0}^J x_i^2$, where m is the regression parameter. If $m \notin \sigma(-A)$ then $\mathbf{x}_0 := (x_0, x_1, \dots, x_J)^T = (mI + A)^{-1}b$ satisfies $F(\mathbf{x}_0; m) = \min_{\mathbf{x} \in \mathbb{R}^{J+1}} F(\mathbf{x}; m)$ where $A_{(J+1) \times (J+1)}$, $mI_{(J+1) \times (J+1)}$ and $b_{(J+1) \times 1}$ are defined as follows:

$$A = \begin{bmatrix} (T-J-1) & \sum_{t=J}^{T-2} f(t-1) & \dots & \sum_{t=J}^{T-2} f(t-J) \\ \sum_{t=J}^{T-2} f(t-1) & \sum_{t=J}^{T-2} f(t-1)^2 & \dots & \sum_{t=J}^{T-2} f(t-1)f(t-J) \\ \vdots & \vdots & \ddots & \vdots \\ \sum_{t=J}^{T-2} f(t-J) & \sum_{t=J}^{T-2} f(t-J)f(t-1) & \dots & \sum_{t=J}^{T-2} f(t-J)^2 \end{bmatrix},$$

$$mI = \begin{bmatrix} m & 0 & 0 & \dots & 0 \\ 0 & m & 0 & \dots & 0 \\ 0 & 0 & m & \dots & 0 \\ \vdots & \vdots & \vdots & \ddots & \vdots \\ 0 & 0 & \dots & \dots & m \end{bmatrix}, \quad b = \begin{bmatrix} \sum_{t=J}^{T-2} f(t) \\ \sum_{t=J}^{T-2} f(t)f(t-1) \\ \sum_{t=J}^{T-2} f(t)f(t-2) \\ \vdots \\ \sum_{t=J}^{T-2} f(t)f(t-J) \end{bmatrix}.$$

Proof: It is easily to see that if $F(\mathbf{x}_0; m) = \min_{\mathbf{x} \in \mathbb{R}^{J+1}} F(\mathbf{x}; m)$ then $\frac{\partial}{\partial x_j} F(\mathbf{x}_0; m) = 0 \quad \forall j = 0 \dots J$. Hence at the minimal point \mathbf{x}_0 we have:

$$\begin{aligned} \frac{\partial}{\partial x_0} F(\mathbf{x}_0; m) &= \frac{\partial}{\partial x_0} \left[\sum_{t=J}^{T-2} (f(t) - \hat{f}(t))^2 + m \sum_{i=0}^J x_i^2 \right] \\ &= -2 \sum_{t=J}^{T-2} [(f(t) - (x_0 + x_1 f(t-1) + \dots + x_J f(t-J))) \cdot 1] \\ &\quad + 2mx_0, \\ \frac{\partial}{\partial x_j} F(\mathbf{x}_0; m) &= \frac{\partial}{\partial x_j} \left[\sum_{t=J}^{T-2} (f(t) - \hat{f}(t))^2 + m \sum_{i=0}^J x_i^2 \right] \\ &= -2 \sum_{t=J}^{T-2} [(f(t) - (x_0 + x_1 f(t-1) + \dots + x_J f(t-J))) \cdot f(t-j)] \\ &\quad + 2mx_j, \quad j = 1, 2, \dots, J. \end{aligned}$$

Thus we easily obtain the following results:

$$\begin{aligned} \sum_{t=J}^{T-2} f(t) &= \sum_{t=J}^{T-2} (x_0 + x_1 f(t-1) + \dots + x_J f(t-J)) + mx_0, \\ \sum_{t=J}^{T-2} f(t) &= \sum_{t=J}^{T-2} (x_0 + x_1 f(t-1) + \dots + x_J f(t-J)) \cdot f(t-j) \\ &\quad + mx_j, \quad j \neq 0. \end{aligned}$$

$$\Rightarrow \begin{bmatrix} (T-J-1) + m & \sum_{t=J}^{T-2} f(t-1) & \dots & \sum_{t=J}^{T-2} f(t-J) \\ \sum_{t=J}^{T-2} f(t-1) & \sum_{t=J}^{T-2} f(t-1)^2 + m & \dots & \sum_{t=J}^{T-2} f(t-1)f(t-J) \\ \vdots & \vdots & \ddots & \vdots \\ \sum_{t=J}^{T-2} f(t-J) & \sum_{t=J}^{T-2} f(t-J)f(t-1) & \dots & \sum_{t=J}^{T-2} f(t-J)^2 + m \end{bmatrix} \begin{bmatrix} x_0 \\ x_1 \\ \vdots \\ x_J \end{bmatrix}$$

$$= \begin{bmatrix} \sum_{t=J}^{T-2} f(t) \\ \sum_{t=J}^{T-2} f(t)f(t-1) \\ \vdots \\ \sum_{t=J}^{T-2} f(t)f(t-J) \end{bmatrix}$$

$$\Rightarrow (x_0, x_1, \dots, x_J)^T = (mI + A)^{-1}b \text{ if } m \notin \sigma(-A).$$

This completes the proof. \blacksquare

Remark 2.1 We note that, for giving a regression parameter $m > 0$, the cost function F is positive of degree 2 with respect to each x_j and $F(\mathbf{x}; m) \rightarrow \infty$ as $x_j \rightarrow \pm\infty$, $\mathbf{x} = (x_0, x_1, \dots, x_J)$. It follows that $F(\mathbf{x}_0; m) = \min_{\mathbf{x} \in \mathbb{R}^{J+1}} F(\mathbf{x}; m)$ if and only if $\frac{\partial}{\partial x_j} F(\mathbf{x}_0; m) = 0 \quad \forall j = 0 \dots J$.

From Theorem II.2 we have the following numerical **Algorithm 2.1**.

Algorithm 1: Normal Gradient Equation

Input: Training Data $\{f(t), 0 \leq t \leq T-2\}$;

Regularization Parameter m ; Order of FIR J .

Compute A, b of $(mI + A)\mathbf{x} = b$ with cost function and ridge regularization as theorem above.

Choose $m \notin \sigma(-A)$ if not change m .

Solve $\mathbf{x} = (mI + A)^{-1}b$.

return Weights of FIR Model: $\mathbf{x} = \{x_i, 0 \leq i \leq J\}$

2) *Option for the Orders of FIR filters:* In order to find the appropriate orders for training each FIR models $(\hat{\beta}(t), \hat{\gamma}_1(t), \hat{\gamma}_2(t), \hat{\eta}_1(t), \hat{a}_3(t))$, we divide the parameters data $\{\beta(t), \gamma_1(t), \gamma_2(t), \eta_1(t), a_3(t), 0 \leq t \leq T-2\}$ into respective two parts, the training data set (size: ℓ_T) and the validation set (size: ℓ_V) where $\ell_V = T-1-\ell_T$.

Algorithm 2: Order Searcher

Input: Data: $\{f(t), 0 \leq t \leq T-2\}$; Training size: ℓ_T ;

Lower Bound of Order: L_J ; Upper Bound of Order: U_J ;

Regularization Parameter: m .

Divide the data into Training Set:

$Data_T := \{f(t), 0 \leq t \leq \ell_T - 1\}$, and Validation Set:

$Data_V := \{f(t), \ell_T \leq t \leq T-2\}$.

Compute Validation Length: ℓ_V .

for $J \leftarrow L_J$ **to** U_J **do**

while $\ell_T \leq t \leq T-2$ **do**

 Train model with (9), J, m and $Data_T$ by Algorithm 1

 1

 Estimate $\hat{f}_J(t)$, then Append to Predicting set

$Pred_V(J) := \{\hat{f}_J(t), \ell_T \leq t \leq T-2\}$ of Validation.

end while

 Calculate $err(J) := \sum_t |Pred_V(J) - Data_V| =$

$\sum_{t=\ell_T}^{T-2} |\hat{f}_J(t) - f(t)|$, then Append to Error Set

$Error := \{err(J), L_J \leq J \leq U_J\}$.

end for

$J_{fit} = \arg \min_{\{J\}} [Error]$.

return Orders of FIR: J_{fit} .

By using the training set for fitting the model, we take the prediction with the same length as the validation set for

different orders on certainly suitable range ($[L_J, U_J] \subseteq \mathbb{N}$). After this step, we can find the argument of the minimum for the sums of errors w.r.t each orders J as follows

$$\arg \min_{\{J\}} \left[\sum_{t=\ell_T}^{T-2} |\hat{f}_J(t) - f(t)| \right], \quad L_J \leq J \leq U_J.$$

The Algorithm 2 is the implementing details about the searching method of orders.

For FIG. 6 ~ FIG. 19 in Section 4, after obtaining the orders of respective FIR filters, we will apply the certain range $T - \ell_V \leq t \leq T - 1$ of the validation data to conduct the 5%, 10% and 20% effective intervals which are the respective error between prediction and true value for the forecast.

3) *Main Algorithm*: Firstly, we apply Algorithm 1 to train model (8) for obtaining $\hat{\beta}(t), \hat{\gamma}_1(t), \hat{\gamma}_2(t), \hat{\eta}_1(t)$ and $\hat{a}_3(t)$. Secondly, by using the following, we can estimate $\hat{Q}(t), \hat{I}(t), \hat{A}(t), \hat{R}(t), \hat{D}(t)$ for $t \geq T - 1$:

Algorithm 3: Tracking Multiple SQIARD Models

Input: Data:
 $\{Q(t), I(t), A(t), R(t), D(t), 0 \leq t \leq T - 1\}$;
 Regularization Parameters: m_1, m_2, m_3, m_4, m_5 ; Orders of
 FIR: J_1, J_2, J_3, J_4, J_5 ; Criteria: P.
 Calculate $\{\beta(t), \gamma_1(t), \gamma_2(t), \eta_1(t), a_3(t), 0 \leq t \leq T - 2\}$
 by (6) and append to $\mathcal{B}, \Gamma_1, \Gamma_2, \mathcal{H}, \mathcal{A}$, respectively.
 Train models with (9); $J_i, 1 \leq i \leq 5; m_i, 1 \leq i \leq 5$ and
 $\mathcal{B}, \Gamma_1, \Gamma_2, \mathcal{H}, \mathcal{A}$, respectively by Algorithm 1
 Estimate
 $\hat{\beta}(T - 1), \hat{\gamma}_1(T - 1), \hat{\gamma}_2(T - 1), \hat{\eta}_1(T - 1), \hat{a}_3(T - 1)$ by
 (8), and append to $\mathcal{B}, \Gamma_1, \Gamma_2, \mathcal{H}, \mathcal{A}$, respectively.
 Estimate $\hat{Q}(T), \hat{I}(T), \hat{A}(T), \hat{R}(T), \hat{D}(T)$ by (10).
while $T \leq t \leq T + P$ **do**
 Train models with (9); $J_i, 1 \leq i \leq 5; m_i, 1 \leq i \leq 5$
 and $\mathcal{B}, \Gamma_1, \Gamma_2, \mathcal{H}, \mathcal{A}$, respectively by Algorithm 1.
 Estimate $\hat{\beta}(t), \hat{\gamma}_1(t), \hat{\gamma}_2(t), \hat{\eta}_1(t), \hat{a}_3(t)$ by (8), and
 append to $\mathcal{B}, \Gamma_1, \Gamma_2, \mathcal{H}, \mathcal{A}$, respectively.
 Estimate
 $\hat{Q}(t + 1), \hat{I}(t + 1), \hat{A}(t + 1), \hat{R}(t + 1), \hat{D}(t + 1)$ by (10).
end while
return Appended training data set: $\mathcal{B}, \Gamma_1, \Gamma_2, \mathcal{H}, \mathcal{A}$;
 Predictions of Q, I, A, R, D :
 $\{\hat{Q}(t), \hat{I}(t), \hat{A}(t), \hat{R}(t), \hat{D}(t), T \leq t \leq T + P\}$.

$$\begin{cases} \hat{S}(t + 1) = S(t) - \frac{\beta(t)S(t)(I(t) + \delta A(t))}{S(t) + I(t) + A(t)} + a_3(t)\mu_2 Q(t) \\ \hat{Q}(t + 1) = Q(t) + \frac{\beta(t)S(t)(I(t) + \delta A(t))}{S(t) + I(t) + A(t)} \\ \quad - (a_1(t)\mu_1 + a_2(t)\mu_1 + a_3(t)\mu_2)Q(t) \\ \hat{I}(t + 1) = I(t) + a_1(t)\mu_1 Q(t) - \gamma_1(t)I(t) - \eta_1(t)I(t) \\ \hat{A}(t + 1) = A(t) + a_2(t)\mu_1 Q(t) - \gamma_2(t)A(t) - \eta_2(t)A(t) \\ \hat{R}(t + 1) = R(t) + \gamma_1(t)I(t) + \gamma_2(t)A(t) \\ \hat{D}(t + 1) = D(t) + \eta_1(t)I(t) + \eta_2(t)A(t). \end{cases} \quad (10)$$

We assume the period of COVID-19 is finite. Then we can append the prediction $\hat{\beta}(t), \hat{\gamma}_1(t), \hat{\gamma}_2(t), \hat{\eta}_1(t), \hat{a}_3(t), \geq T - 1$ to increase the variety of training set.

Definition. (Appended Training Data Set)

Let $f(t), 0 \leq t \leq T - 2$ be the training set, $\hat{f}(t), t \geq T - 1$ be the prediction depend on the trained model and P be the stopping criteria of the forecast. Then the Appended Training Data defined as: $\mathcal{F} := \{\mathcal{F}(t) | (\mathcal{F}(t) = f(t), \text{ if } 0 \leq t \leq T - 2) \text{ or } (\mathcal{F}(t) = \hat{f}(t), \text{ if } T - 1 \leq t \leq T + P)\}$, e.g., the Appended training data set of $\beta, \mathcal{B} := \{\mathcal{B}(t) | (\mathcal{B}(t) = \beta(t), \text{ if } 0 \leq t \leq T - 2) \text{ or } (\mathcal{B}(t) = \hat{\beta}(t), \text{ if } T - 1 \leq t \leq T + P)\}$. Similarly we have $(\gamma_1, \Gamma_1), (\gamma_2, \Gamma_2), (\eta_1, \mathcal{H}), (a_3, \mathcal{A})$.

Before conducting the tracking Algorithm 3, we already obtain the respective order of $\hat{\beta}, \hat{\gamma}_1, \hat{\gamma}_2, \hat{\eta}_1, \hat{a}_3$ by Algorithm 2 and the effective intervals for the forecast.

C. Stability Analysis of Equilibrium

In this section, we will propose the relation between the basic reproduction number and the stability of equilibrium for the SQIARD model with constant parameter coefficients. First, we have the following asymptotic behavior of solutions.

Theorem II.3. For each solution of the SQIARD model with constant parameters coefficients satisfies $S(t) \rightarrow S_\infty \geq 0, Q(t) \rightarrow 0, I(t) \rightarrow 0, A(t) \rightarrow 0, R(t) \rightarrow R_\infty > 0, D(t) \rightarrow D_\infty > 0$ as $t \rightarrow \infty$.

In order to prove Theorem 2.5, we need the following lemma.

Lemma II.1. Let f be continuously differentiable. If k and $M > 0 \in \mathbb{R}$ such that $\lim_{t \rightarrow \infty} f(t) = k$ and $|f''| \leq M \quad \forall t$, then $\lim_{t \rightarrow \infty} f'(t) = 0$.

Proof: The proof can be found in Coppell (1965, p. 139). ■

Proof: of Theorem II.3. We assume that the quarantine to susceptible population always smaller than the susceptible to quarantine, it means that $S(t)$ is decreasing and $S(t) \downarrow S_\infty \geq 0$. Moreover, $(S + Q)' = -(a_1\mu_1 + a_2\mu_1)Q < 0$, then $Q(t) \downarrow Q_\infty \geq 0$. We also have $N = S(t) + Q(t) + I(t) + A(t) + R(t) + D(t)$ with $R' \geq 0$ and $D' \geq 0$, it implies $R_\infty > 0$ and $D_\infty > 0$. Furthermore $R'' = \gamma_1 I' + \gamma_2 A'$, $|I'|$ and $|A'|$ are bounded, there exists $M > 0$ such that $|R''| \leq M$. Therefore, by lemma II.1, $I(t) \rightarrow I_\infty = 0$ and $A(t) \rightarrow A_\infty = 0$ as $t \rightarrow \infty$.

To verify $Q_\infty = 0$, we may assume $Q_\infty > 0$. Since $I' = a_1\mu_1 Q - (\gamma_1 + \eta_1)I = 0$ and $I_\infty = 0$, then $a_1\mu_1 Q_\infty = 0(\rightarrow \leftarrow)$. ■

Now we consider the limiting system of the model in (1) as follows. Let $W_1 = \frac{S}{I}, W_2 = \frac{A}{I}, W_3 = \frac{Q}{I}$. then the above system in (1) can be reduced to

$$\begin{aligned}
W_1' &= \frac{S'I - SI'}{I^2} = \frac{-\beta(1 + \delta W_2)}{1 + W_1 + W_2} W_1 + a_3 \mu_2 W_2 \\
&\quad - W_1 (a_1 \mu_1 W_3 - (\gamma_1 + \eta_1)) \\
W_2' &= \frac{A'I - AI'}{I^2} = a_2 \mu_1 W_3 - (\gamma_2 + \eta_2) W_2 \\
&\quad - W_2 (a_1 \mu_1 W_3 - (\gamma_1 + \eta_1)) \\
W_3' &= \frac{Q'I - QI'}{I^2} = \frac{\beta(1 + \delta W_2)}{1 + W_1 + W_2} W_1 \\
&\quad - q W_3 - W_3 (a_1 \mu_1 W_2 - (\gamma_1 + \eta_1))
\end{aligned} \tag{11}$$

We discuss the stability of respective equilibrium of system (11):

Case 1. $E_0 = (0, 0, 0)$ which always exists. The variational matrix is

$$M_0 = \begin{bmatrix} -\beta + (\gamma_1 + \eta_1) & 0 & a_3 \mu_2 \\ 0 & -(\gamma_2 + \eta_2) + (\gamma_1 + \eta_1) & a_2 \mu_1 \\ \beta & 0 & -q + (\gamma_1 + \eta_1) \end{bmatrix}$$

The eigenvalues are:

$$\begin{aligned}
\lambda_1 &= (\gamma_1 + \eta_1) - (\gamma_2 + \eta_2) \\
\lambda_2 &= \frac{\beta + q - 2(\gamma_1 + \eta_1) + \sqrt{(\beta - q)^2 + 4a_3\beta\mu_2}}{2} \\
\lambda_3 &= \frac{\beta + q - 2(\gamma_1 + \eta_1) - \sqrt{(\beta - q)^2 + 4a_3\beta\mu_2}}{2}
\end{aligned}$$

E_0 is asymptotically stable if all eigenvalues are negative, that is to say

$$\left\{ \begin{array}{l} (\gamma_1 + \eta_1) < (\gamma_2 + \eta_2) \\ \beta > \frac{(\gamma_1 + \eta_1)(\gamma_1 + \eta_1 - q)}{-q + (\gamma_1 + \eta_1) + a_3\mu_2}, \\ \text{if } -q + (\gamma_1 + \eta_1) + a_3\mu_2 < 0 \text{ and } \beta < -q + 2(\gamma_1 + \eta_1) \\ \beta < \frac{(\gamma_1 + \eta_1)(\gamma_1 + \eta_1 - q)}{-q + (\gamma_1 + \eta_1) + a_3\mu_2}, \\ \text{if } -q + (\gamma_1 + \eta_1) + a_3\mu_2 > 0 \text{ and } \beta < -q + 2(\gamma_1 + \eta_1) \end{array} \right.$$

Case 2. $E_\infty = (\infty, \tilde{W}_2, \tilde{W}_3)$,

From the equation W_1' , we have $\frac{W_1'}{W_1} \leq -a_1 \mu_1 W_3 + (\gamma_1 + \eta_1)$, then $\tilde{W}_3 \leq \frac{\gamma_1 + \eta_1}{a_1 \mu_1}$ if $\lim_{t \rightarrow \infty} W_1(t) = \infty$

From the equation W_2', W_3' , and $\lim_{t \rightarrow \infty} W_1(t) = \infty$, then it can be shown that $(\tilde{W}_2, \tilde{W}_3)$ is the solution of

$$a_2 \mu_1 W_3 - (\gamma_2 + \eta_2) W_2 - W_2 (a_1 \mu_1 W_3 - (\gamma_1 + \eta_1)) = 0$$

$$\beta(1 + \delta W_2) - q W_3 - W_3 (a_1 \mu_1 W_2 - (\gamma_1 + \eta_1)) = 0$$

To investigate in further details, we go back to the limiting system in (11). We using the **Poincare transform** to pull back from infinity. Let $Z_1 = \frac{1}{W_1}, Z_2 = \frac{W_2}{W_1}, Z_3 = \frac{W_3}{W_1}$, and $q =$

$$a_1 \mu_1 + a_2 \mu_1 + a_3 \mu_2$$

$$\begin{aligned}
Z_1' &= \frac{I'S - IS'}{S^2} = a_1 \mu_1 Z_3 - (\gamma_1 + \eta_1) Z_1 \\
&\quad - Z_1 \left(\frac{-\beta(Z_1 + \delta Z_2)}{1 + Z_1 + Z_2} + a_3 \mu_2 Z_3 \right) \\
Z_2' &= \frac{A'S - AS'}{S^2} = a_2 \mu_1 Z_3 - (\gamma_2 + \eta_2) Z_2 \\
&\quad - Z_2 \left(\frac{-\beta(Z_1 + \delta Z_2)}{1 + Z_1 + Z_2} + a_3 \mu_2 Z_3 \right) \\
Z_3' &= \frac{Q'S - QS'}{S^2} = \beta \frac{(Z_1 + \delta Z_2)}{1 + Z_1 + Z_2} - q Z_3 \\
&\quad - Z_3 \left(\frac{-\beta(Z_1 + \delta Z_2)}{1 + Z_1 + Z_2} + a_3 \mu_2 Z_3 \right)
\end{aligned} \tag{12}$$

The local stability of E_∞ of system (12) is equivalent to the local stability of $E_0 = (0, 0, 0)$ of system (11). We have the following theorem.

Theorem II.4. E_∞ is stable $\iff \beta < \frac{D_1 D_2}{a_1 D_2 + a_2 \delta D_1} \iff R_Q < 1$, where $D_1 = (\gamma_1 + \eta_1)$ and $D_2 = (\gamma_2 + \eta_2)$.

Proof: Let the variation matrix is

$$\tilde{M}_0 = \begin{bmatrix} -D_1 & 0 & a_1 \mu_1 \\ 0 & -D_2 & a_2 \mu_1 \\ \beta & \beta \delta & -q \end{bmatrix},$$

By using the similar proof of Theorem II.1, we can easily get the conclusion of Theorem II.4. ■

In the following, we will use Lyapunov function theory to explore the relation between the globally asymptotical stability of equilibrium and R_Q .

Theorem II.5. If $\beta < \min\{\gamma_1 + \eta_1, \frac{\gamma_2 + \eta_2}{\delta}\}$, then $R_Q < 1$ and the disease-free equilibrium $E^* = (S^*, 0, 0, 0)$ is globally asymptotically stable of (1).

Proof: Consider the following Lyapunov function

$$V_{E^*} = S^* r\left(\frac{S}{S^*}\right) + Q + I + A, \text{ where } r(x) = x - 1 - \ln(x).$$

We want to show that $\dot{V}_{E^*} < 0$. By assumption in Theorem II.5, it is easily to obtain

$$\begin{aligned}
\frac{dV_{E^*}}{dt} &= \frac{\beta S^*(I + \delta A)}{S + I + A} - \frac{S^*}{S} a_3 \mu_2 Q - (\gamma_1 + \eta_1) I - (\gamma_2 + \eta_2) A \\
&= -\frac{S^*}{S} a_3 \mu_2 Q + \left(\frac{\beta S^*}{S + I + A} - (\gamma_1 + \eta_1) \right) I + \left(\frac{\beta S^* \delta}{S + I + A} - (\gamma_2 + \eta_2) \right) A \\
&< -\frac{S^*}{S} a_3 \mu_2 Q + (\beta - (\gamma_1 + \eta_1)) I + (\beta \delta - (\gamma_2 + \eta_2)) A \\
&< 0.
\end{aligned}$$

Hence, the disease-free equilibrium E^* is globally asymptotically stable of (1).

Now, we want to show that $R_Q < 1$. Since $\beta < \min\{\gamma_1 +$

$$\eta_1, \frac{\gamma_2 + \eta_2}{\delta}\}, \frac{\beta}{\gamma_1 + \eta_1} < 1 \text{ and } \frac{\beta\delta}{\gamma_2 + \eta_2} < 1,$$

$$R_Q = \frac{(a_1 + a_2)\mu_1}{a_1\mu_1 + a_2\mu_1 + a_3\mu_2} \left(\frac{a_1\beta}{a_1 + a_2} + \frac{a_2\beta\delta}{a_1 + a_2} \right) < \frac{\mu_1}{a_1\mu_1 + a_2\mu_1 + a_3\mu_2} < 1.$$

We complete the proof. ■

We discuss the relation between the parameters of the model as follows:

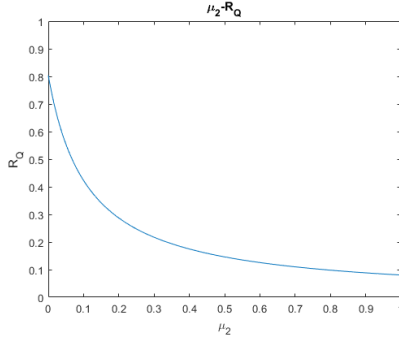


Fig. 2. $\mu_2 - R_Q$

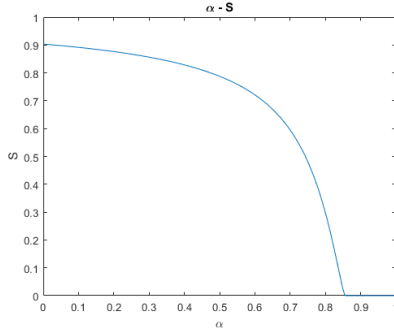


Fig. 3. $\alpha - S$

For Figure 2, given $\beta = 0.080; \delta = 0.5; a_1 = 0.04; a_2 = 0.06; a_3 = 0.9; \eta_1 = 0.01; \eta_2 = 0; \gamma_1 = 0.06; \gamma_2 = 0.06; \mu_1 = 1; S_0 = 1000; I_0 = 10; A_0 = Q_0 = R_0 = D_0 = 0$. We want to observe the relation of μ_2 and R_Q . By Figure 2, while the value of μ_2 increases, R_Q decreases. That is, when the μ_2 increases faster, the epidemic will be controlled better.

For Figure 3, given $\beta = 0.27; \delta = 0.5; a_3 = 0; \eta_1 = 0.01; \eta_2 = 0; \gamma_1 = 0.06; \gamma_2 = 0.06; \mu_1 = 1; \mu_2 = 1; S_0 = 1000; I_0 = 10; A_0 = Q_0 = R_0 = D_0 = 0$, and $\alpha = a_1/(a_1 + a_2)$. We want to observe the relation of α and S . By Figure 3, while the value of α increases, S decreases. That is, if the proportion of infector is higher, the number of people in S will be lower at the end of the epidemic, even all people will be infected. Contrarily, if the proportion of asymptomatic people is relatively high, the epidemic may infect a small group of people eventually.

III. SIARD MODEL

In the previous section, we established and discussed the SQIARD model. However, data on the number of people quarantined daily in most countries is not easy to obtain no, and only a few countries have open data (such as the United States). Therefore, in this section we will simplify the parameter $Q(t)$ to build a new model.

A. The Derivation and Basic Reproduction Number

In order to verify the epidemic effect of prediction of the SIARD model, we will take the following two steps:

- 1) Remove the parameter $Q(t)$, and simplify the SQIARD infectious disease mathematical model under the other assumptions unchanged. Use the same training method to train the SIARD model and observe its effect of prediction .
- 2) Use data from countries that have “data on daily quarantine population” to compare the effect of prediction s of the two models on the epidemic.

The variables are given as follows: [S : susceptible population; I : infective population; A : asymptomatic infective population; R : recovered population; D : deaths]. The model

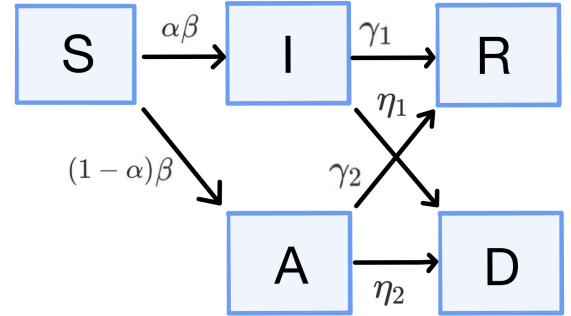


Fig. 4. The flow chart of SIARD

parameters are given as follows: [β : the progression rate of susceptible class to infective classes; δ : the reduction in infectiousness of asymptomatic infectives, where $0 < \delta < 1$; α : the fraction of susceptible from susceptible to I or A , where $0 < \alpha < 1$; γ_1 and γ_2 : the recovered rates of infective classes I and A ; η_1 and η_2 : are the disease death rates of infective classes I and A].

$$\begin{aligned} S' &= -\frac{\beta S(I + \delta A)}{S + I + A} \\ I' &= \alpha \frac{\beta S(I + \delta A)}{S + I + A} - \gamma_1 I - \eta_1 I \\ A' &= (1 - \alpha) \frac{\beta S(I + \delta A)}{S + I + A} - \gamma_2 A - \eta_2 A \\ R' &= \gamma_1 I + \gamma_2 A \\ D' &= \eta_1 I + \eta_2 A \end{aligned} \quad (13)$$

$S(0) = S_0 > 0$, $I(0) = I_0 > 0$, $A(0) = A_0 > 0$, $R(0) = 0$ and $D(0) = 0$.

We note that $S(t) + I(t) + A(t) + R(t) + D(t) = N =$

$S_0 + I_0 + A_0$ where N is the total population. To further examine the stability condition of such a system, we let

$$R_0 = \alpha \frac{\beta}{\gamma_1 + \eta_1} + (1 - \alpha) \frac{\beta\delta}{\gamma_2 + \eta_2}$$

Note that R_0 is simply the basic reproduction number of this system.

Due to the COVID-19 data is uploaded in days, we revise the differential equation into discrete time difference equation.

$$\begin{aligned} S(t+1) - S(t) &= -\frac{\beta S(I + \delta A)}{S + I + A} \\ I(t+1) - I(t) &= \alpha \frac{\beta S(I + \delta A)}{S + I + A} - \gamma_1 I - \eta_1 I \\ A(t+1) - A(t) &= (1 - \alpha) \frac{\beta S(I + \delta A)}{S + I + A} - \gamma_2 A - \eta_2 A \\ R(t+1) - R(t) &= \gamma_1 I + \gamma_2 A \\ D(t+1) - D(t) &= \eta_1 I + \eta_2 A \end{aligned} \quad (14)$$

When the disease first spreads, the number of people infected is much smaller than the total population, the number of suspected infections is approximated to the total of population. Then above equations can simplified as follows :

$$\begin{aligned} I(t+1) - I(t) &= \alpha\beta(I + \delta A) - \gamma_1 I - \eta_1 I \\ A(t+1) - A(t) &= (1 - \alpha)\beta(I + \delta A) - \gamma_2 A - \eta_2 A \end{aligned} \quad (15)$$

Write above formula in the matrix form yields the following equation:

$$\begin{bmatrix} I(t+1) \\ A(t+1) \end{bmatrix} =$$

$$\begin{bmatrix} 1 + \alpha\beta - (\gamma_1 + \eta_1) & \alpha\beta\delta \\ (1 - \alpha)\beta & 1 + (1 - \alpha)\beta\delta - (\gamma_2 + \eta_2) \end{bmatrix} \begin{bmatrix} I(t) \\ A(t) \end{bmatrix} \quad (16)$$

Let

$$\mathbf{A} = \begin{bmatrix} 1 + \alpha\beta - (\gamma_1 + \eta_1) & \alpha\beta\delta \\ (1 - \alpha)\beta & 1 + (1 - \alpha)\beta\delta - (\gamma_2 + \eta_2) \end{bmatrix}$$

be the transmission matrix of the above system equations. It's well know such a system is stable if the spectral radius of \mathbf{A} is less than 1. In other words, $I(t+1)$ and $A(t+1)$ will converge asymptotically to finite constant when $t \rightarrow \infty$. In the following theorem, we show that there is no outbreak if $R_0 < 1$ and there is an outbreak if $R_0 > 1$. Thus, R_0 is known as the threshold for an outbreak in such a model.

Theorem III.1. $R_0 < 1$ if and only if $\rho(\mathbf{A}) < 1$

Proof: First, we prove the sufficient condition. It's easy to show that \mathbf{A} is positive matrix. Therefore, by **Perron-Frobenius Theorem**, we have $\rho(\mathbf{A}) \in \sigma(\mathbf{A})$, and $\sigma(\mathbf{A}) \subseteq \mathbb{R}$. Let $\lambda_1 \geq \lambda_2$ and $\tilde{\lambda}_i = \lambda_i - 1, i = 1, 2$, then $\tilde{\lambda}_i \in \sigma(\mathbf{A})$ and $\lambda_1 \geq \lambda_2$, where

$$\mathbf{A} - \mathbf{I} = \tilde{\mathbf{A}} = \begin{bmatrix} \alpha\beta - (\gamma_1 + \eta_1) & \alpha\beta\delta \\ (1 - \alpha)\beta & (1 - \alpha)\beta\delta - (\gamma_2 + \eta_2) \end{bmatrix}$$

Let

$$\begin{aligned} z_1 &= \text{tr}(\tilde{\mathbf{A}}) \\ &= \alpha\beta - (\gamma_1 + \eta_1) + (1 - \alpha)\beta\delta - (\gamma_2 + \eta_2), \\ z_2 &= -|\tilde{\mathbf{A}}| \\ &= -\{[\alpha\beta - (\gamma_1 + \eta_1)][(1 - \alpha)\beta\delta - (\gamma_2 + \eta_2)]\} \\ &\quad + (1 - \alpha)\beta\alpha\beta\delta \end{aligned} \quad (17)$$

We have $\tilde{\lambda}_1 = \frac{1}{2}(z_1 + \sqrt{z_1^2 + 4z_2})$ and $\tilde{\lambda}_2 = \frac{1}{2}(z_1 - \sqrt{z_1^2 + 4z_2})$. If $R_0 < 1$, we can obtain $z_2 < 0$, $\frac{\alpha\beta}{\gamma_1 + \eta_1} < 1$ and $\frac{(1 - \alpha)\beta\delta}{\gamma_2 + \eta_2} < 1$. It is easy to see that $z_1 < 0$ and $\tilde{\lambda}_1 < \frac{1}{2}(z_1 + |z_1|) = 0$, that is $\lambda_1 - 1 < 0$, i.e. $\lambda_1 < 1$. This shows that $\rho(\mathbf{A}) < 1$.

The proof of necessary condition is similar with Theorem II.1. Let $\rho(\mathbf{A}) < 1$, then $\tilde{\lambda}_i \in \sigma(\tilde{\mathbf{A}})$ and $\tilde{\lambda}_i < 0, i = 1, 2$. It implies $\tilde{\mathbf{A}}$ is stable. Using a method of Theorem II.1, we can easily get $R_0 < 1$. ■

The following Corollary will show the link between R_0 and the outbreak of the epidemic.

Corollary III.1. If $R_0 < 1$ then there is no outbreak of the epidemic. Moreover, if $R_0 > 1$, then there is an outbreak of epidemic.

Proof: The proof is similar to Corollary II.1. ■

B. Tracking Time-Depend SIARD Model Algorithms

For the SIARD, $\beta(t), \gamma_1(t), \gamma_2(t), \eta_1(t)$ can be evolved as (18) from the discrete form of the SIARD differential equation.

$$\begin{aligned} \beta(t) &= \frac{S(t) - S(t+1)}{S(t)(I(t) + \delta A(t))} (S(t) + I(t) + A(t)) \\ \gamma_1(t) &= (1 + \frac{D(t+1) - D(t)}{I(t)}) + \alpha \frac{S(t) - S(t+1)}{I(t)} - \frac{I(t+1)}{I(t)} \\ \gamma_2(t) &= 1 + (1 - \alpha) \frac{S(t) - S(t+1)}{A(t)} - \frac{A(t+1)}{A(t)} \\ \eta_1(t) &= \frac{D(t+1) - D(t)}{I(t)} \end{aligned} \quad (18)$$

Similarly, in order to estimating $\hat{I}(t), \hat{A}(t), \hat{R}(t), \hat{D}(t)$ with SIARD for $t > T$, we use the Algorithm 1 to train models of (8) without \hat{a}_3 and obtain $\hat{\beta}(t), \hat{\gamma}_1(t), \hat{\gamma}_2(t), \hat{\eta}_1(t)$. Then, we use it to compute $\hat{I}(t), \hat{A}(t), \hat{R}(t), \hat{D}(t)$ as (19) and also append the prediction $\hat{\beta}(t), \hat{\gamma}_1(t), \hat{\gamma}_2(t), \hat{\eta}_1(t), t \geq T - 1$ to

$\mathcal{B}, \Gamma_1, \Gamma_2, \mathcal{H}$ respectively.

$$\begin{cases} \hat{S}(t+1) = S(t) - \frac{\beta(t)S(t)(I(t) + \delta A(t))}{S(t) + I(t) + A(t)} \\ \hat{I}(t+1) = I(t) + \alpha \frac{\beta(t)S(t)(I(t) + \delta A(t))}{S(t) + I(t) + A(t)} - \gamma_1(t)I(t) - \eta_1(t)I(t) \\ \hat{A}(t+1) = A(t) + (1 - \alpha) \frac{\beta(t)S(t)(I(t) + \delta A(t))}{S(t) + I(t) + A(t)} - \gamma_2(t)A(t) - \eta_2(t)A(t) \\ \hat{R}(t+1) = R(t) + \gamma_1(t)I(t) + \gamma_2(t)A(t) \\ \hat{D}(t+1) = D(t) + \eta_1(t)I(t) + \eta_2(t)A(t), \end{cases} \quad (19)$$

where $t \geq T - 1$. Also, before implementing the Tracking Algorithm, we have to conduct the orders by Algorithm 2 first, then obtaining Tracking SIARD Algorithm from revised Algorithm 3 by removing the $Q(t)$, $\hat{Q}(t)$, $a_3(t)$, $\hat{a}_3(t)$. Section 4 is our result of the forecast.

C. Stability analysis of Equilibrium

In this section, we will propose the relation between the stability of the SIARD model and R_0 . First, we give the following equilibria and their respective stability analyses. We have the following asymptotic behavior as $t \rightarrow \infty$

Theorem III.2. $S(t) \rightarrow S_\infty \geq 0$, $I(t) \rightarrow 0$, $A(t) \rightarrow 0$, $R(t) \rightarrow R_\infty > 0$, $D(t) \rightarrow D_\infty > 0$ as $t \rightarrow \infty$.

Proof: The proof is similar to Theorem II.3 ■

Now we consider the limiting system of the model in (13) as follows. Let $W_1 = \frac{S}{I}$, $W_2 = \frac{A}{I}$, then the system in (13) can be reduced to

$$\begin{aligned} W_1' &= -\beta(1 + \delta W_2) \frac{W_1}{1 + W_1 + W_2} (1 + \alpha W_1) + W_1(\gamma_1 + \eta_1) \\ W_2' &= (1 - \alpha)\beta(1 + \delta W_2) \frac{W_1}{1 + W_1 + W_2} \\ &\quad - \left[\alpha\beta(1 + \delta W_2) \frac{W_1}{1 + W_1 + W_2} + (\gamma_2 + \eta_2) - (\gamma_1 + \eta_1) \right] W_2 \end{aligned} \quad (20)$$

We discuss the equilibria of system (20).

Case 1 : $E_0 = (0, 0)$ always exists. The variation matrix

$$M_0 = \begin{bmatrix} -\beta + \gamma_1 + \eta_1 & 0 \\ (1 - \alpha)\beta & (\gamma_1 + \eta_1) - (\gamma_2 + \eta_2) \end{bmatrix}$$

The eigenvalues are :

$$\lambda_1 = -\beta + \gamma_1 + \eta_1$$

$$\lambda_2 = (\gamma_1 + \eta_1) - (\gamma_2 + \eta_2)$$

And it is asymptotically stable if all the real part of eigenvalues correspond to the variational matrix are negative. Then, in this case, we easily obtain

$$\begin{cases} \beta > \gamma_1 + \eta_1 \\ (\gamma_1 + \eta_1) < (\gamma_2 + \eta_2) \end{cases}$$

Case 2 : $E_2 = (0, W_2^*)$ exists if $(\gamma_1 + \eta_1) - (\gamma_2 + \eta_2) = 0$. The variational matrix $M_2 =$

$$\begin{bmatrix} -\frac{\beta(1 + \delta W_2^*)}{1 + W_2^*} + \gamma_1 + \eta_1 & 0 \\ \frac{(1 - \alpha)\beta(1 + \delta W_2^*)}{1 + W_2^*} - W_2^* \frac{\alpha\beta(1 + \delta W_2^*)}{1 + W_2^*} & (\gamma_1 + \eta_1) - (\gamma_2 + \eta_2) \end{bmatrix}$$

$$\begin{aligned} \lambda_1 &= -\frac{\beta(1 + \delta W_2^*)}{1 + W_2^*} + \gamma_1 + \eta_1 \\ \lambda_2 &= (\gamma_1 + \eta_1) - (\gamma_2 + \eta_2) \end{aligned}$$

And it is stable if eigenvalues are negative.

Because $\lambda_1 < 0$:

$$\lambda_1 = -\frac{\beta(1 + \delta W_2^*)}{1 + W_2^*} + \gamma_1 + \eta_1 < 0$$

$$\Rightarrow -\beta(1 + \delta W_2^*) < -(\gamma_1 + \eta_1)(1 + W_2^*)$$

$$\Rightarrow -\beta - \beta\delta W_2^* < -(\gamma_1 + \eta_1) - (\gamma_1 + \eta_1)W_2^*$$

$$\Rightarrow \beta > \frac{(\gamma_1 + \eta_1)(1 + W_2^*)}{1 + \delta W_2^*}$$

Case 3 : $E_\infty = (\infty, \tilde{W}_2)$

We have $\frac{W_1'}{W_1} = -\beta(1 + \delta W_2) \frac{(1 + \alpha W_1)}{1 + W_1 + W_2} + (\gamma_1 + \eta_1)$

$$\Rightarrow 0 = -\beta(1 + \delta W_2) \frac{(1 + \alpha \tilde{W}_1)}{1 + W_1 + W_2} + (\gamma_1 + \eta_1). \text{ If}$$

$$W_1(t) \rightarrow \infty \Rightarrow \tilde{W}_2 = \frac{\gamma_1 + \eta_1 - \alpha\beta}{\alpha\beta\delta}.$$

To investigate in further details, we go back to limiting system in (20). We using the **Poincare transform** to pull back from infinity, let $Z_1 = \frac{1}{W_1} = \frac{I}{S}$, $Z_2 = \frac{W_2}{W_1} = \frac{A}{S}$.

$$\begin{aligned} Z_1' &= \frac{I'S - IS'}{S^2} \\ &= \alpha\beta \frac{Z_1 + \delta Z_2}{1 + Z_1 + Z_2} - (\gamma_1 + \eta_1)Z_1 + Z_1(\beta \frac{Z_1 + \delta Z_2}{1 + Z_1 + Z_2}) \\ Z_2' &= \frac{A'S - AS'}{S^2} \\ &= (1 - \alpha)\beta \frac{Z_1 + \delta Z_2}{1 + Z_1 + Z_2} - (\gamma_2 + \eta_2)Z_2 + Z_2 \left(\beta \frac{Z_1 + \delta Z_2}{(1 + Z_1 + Z_2)^2} \right) \end{aligned} \quad (21)$$

The local stability of E_∞ of (20) is equivalent to $E_0 = (0, 0, 0)$ of (21).

Theorem III.3. E_∞ is stable $\Leftrightarrow \beta < \frac{D_1 D_2}{\alpha D_2 + (1 - \alpha)\delta D_1} \Leftrightarrow R_0 < 1$, where $D_1 = \gamma_1 + \eta_1$ and $D_2 = \gamma_2 + \eta_2$

Proof: The proof is similar to Theorem II.4. ■

Next, we use the Lyapunov function to explore the relation between the globally asymptotically stability of equilibrium and R_0 .

Theorem III.4. If $\beta < \min\{\gamma_1 + \eta_1, \frac{\gamma_2 + \eta_2}{\delta}\}$ then $R_0 < 1$ and the disease-free equilibrium $E^* = (S^*, 0, 0)$ of system (13) is globally asymptotically stable.

Proof: The proof is similar to Theorem II.5. ■

In our two models (SIARD & SQIARD), we have the respective basic reproduction number R_0, R_Q . The relation between them is as follows :

$$\begin{aligned}
R_Q &= \beta \frac{\mu_1}{a_1\mu_1 + a_2\mu_1 + a_3\mu_2} \left[\frac{a_1}{\gamma_1 + \eta_1} + \frac{a_2\delta}{\gamma_2 + \eta_2} \right] \\
&= \beta \frac{\mu_1}{a_1\mu_1 + a_2\mu_1 + a_3\mu_2} (a_1 + a_2) \left[\frac{\frac{a_1}{a_1+a_2}}{\gamma_1 + \eta_1} + \frac{\frac{a_2}{a_1+a_2}\delta}{\gamma_2 + \eta_2} \right] \\
&= \frac{(a_1\mu_1 + a_2\mu_1)}{a_1\mu_1 + a_2\mu_1 + a_3\mu_2} R_0
\end{aligned}$$

Hence, $R_Q \leq R_0$.

IV. IMPLEMENT AND NUMERICAL ANALYSIS

In this section, we apply SIARD model to US, Brazil, South Korea, India, Russia, Italy, and SQUIARD model to US, then showing the result in each country. In [3], the authors adopted SSE and the method of Markov Chain Monte Carlo to conduct the 95 % confidence intervals for $I(t)$ and $A(t)$, in Mexico from Mar.12 to Jul.2. We implement our SIARD model to make the forecast during the same period in Mexico. Then the result shows that the prediction in [3] is decreasing while the prediction of SIARD is increasing as FIG. IV.

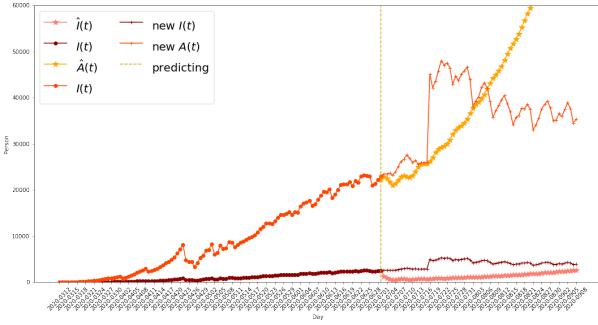


Fig. 5. Mexico.

TABLE I
PARAMETERS FOR SQUIARD AND SIARD (DATE: MAY.11 ~ SEP.8; S_0 :
TOTAL POPULATION; α : THE RATE OF SYMPTOM INFECTED;
 $\beta_o, \gamma_{1o}, \gamma_{2o}, \eta_o$: THE ORDER OF $\beta, \gamma_1, \gamma_2, \eta, a_3$.)

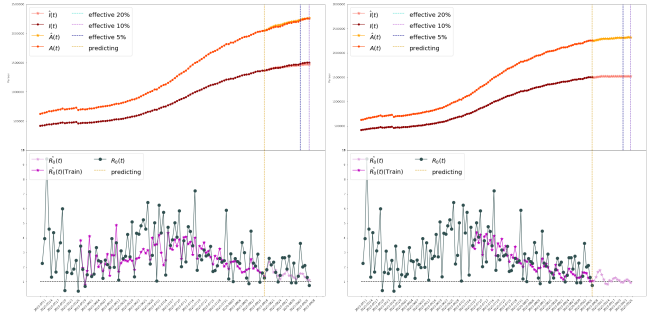
Parameters	S_0	α	β_o	γ_{1o}	γ_{2o}	η_o	a_{3o}
US (SQ)	328200000	0.4	14	8	17	17	10
US (SI)	328200000	0.4	4	17	17	10	None
Brazil (SI)	209500000	0.4	17	12	3	11	None
South Korea (SI)	51640000	0.4	13	15	15	5	None
India (SI)	1353000000	0.4	5	3	3	20	None
Russia (SI)	145500000	0.6	11	19	19	4	None
Italy (SI)	60360000	0.55	13	12	12	19	None

A. Forecast of SQUIARD Model

For the SQUIARD model, we consider the case $\mu_1 = 1$ and $\mu_2 = 1$ where μ_1 and μ_2 are the rate from quarantine to I and A. First, we use 100 data to train model(Phase I in FIG. 6a) and 20 validation data to find the best fitting orders of respective FIR model.(Phase II in FIG. 6a) In US, we obtain the effective intervals with range 16 days in 5 % relative error(Phase III in FIG. 6a) and 20 days in 10 % relative error(Phase IV in FIG. 6a). Secondly, we expand our training data to 120 data(Phase I in FIG. 6b), and then predict for 20 days(Phase II in FIG. 6b). Finally, we apply the effective intervals to the forecast in 16 days(Phase III in FIG. 6b) and 20 days(Phase IV in FIG. 6b).

In FIG. 6a.: Phase I: May. 11 ~ Aug. 19; Phase II: Aug. 19 ~ Sep. 8; Phase III: Aug. 19 ~ Sep. 4; Phase IV: Aug. 19 ~ Sep. 8.

In FIG. 6b.: Phase I: May. 11 ~ Sep. 8; Phase II: Sep. 8 ~ Sep. 28; Phase III: Sep. 8 ~ Sep. 24; Phase III: Sep. 8 ~ Sep. 28.



(a) I, A, R_0 in US. Training size : (b) I, A, R_0 in US. Training size : 120.

Fig. 6. SQUIARD US.

In this case, SQUIARD model was finished in Aug.19, we implement it to conduct the forecast and compare with real data from Aug.20 to Sep.8. (FIG. IV-A).

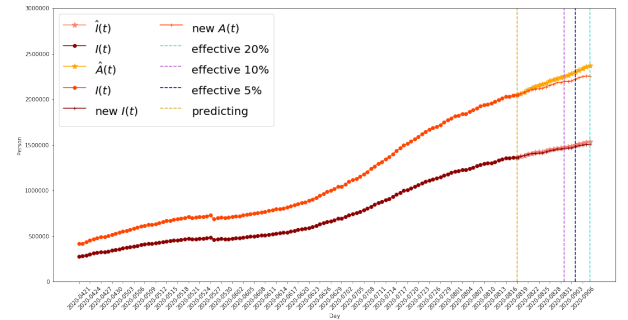


Fig. 7. I, A in US. Date: Apr. 21 ~ Sep. 8. ($a_3, \beta, \gamma_1, \gamma_2, \eta$ are respectively 15, 6, 6, 11, 7.)

B. Forecast of SIARD Model

1) *Fitting the epidemic in US:* For implementing the SIARD model on forecast in US, in the beginning, we apply 100 data to train model(Phase I in FIG. 8a) and 20 validation data(Phase II in FIG. 8a) to compute the effective intervals: 12 days in 5 % relative error(Phase III in FIG. 8a) and 20 days in 10 % relative error(Phase IV in FIG. 8a). Next, we expand our training data to 120 data(Phase I in FIG. 8b) and predict for 20 days(Phase II in FIG. 8b). Finally, we implement the effective intervals on the prediction: 12 days(Phase III in FIG. 8b) and 20 days(Phase IV in FIG. 8b).

In FIG. 8a.: Phase I: May. 11 ~ Aug. 19; Phase II: Aug. 19 ~ Sep. 8; Phase III: Aug. 19 ~ Aug. 31; Phase IV: Aug. 19 ~ Sep. 8.

In FIG. 8b.: Phase I: May. 11 ~ Sep. 8; Phase II: Sep. 8 ~ Sep. 28; Phase III: Sep. 8 ~ Sep. 20; Phase IV: Sep. 8 ~ Sep. 28.

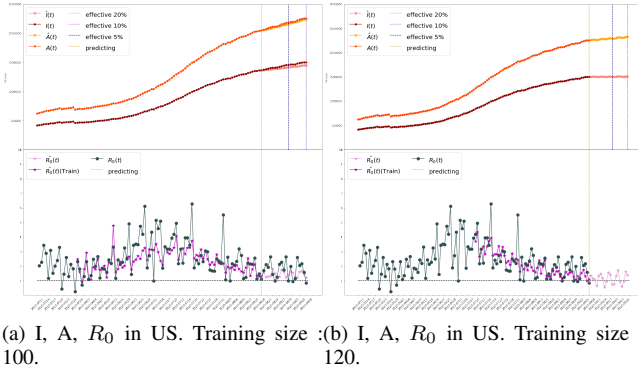


Fig. 8. SIARD US.

In FIG. IV-B1, since SIARD model was also finished in Aug.19, we use it to predict from Aug.20 to Sep.8.

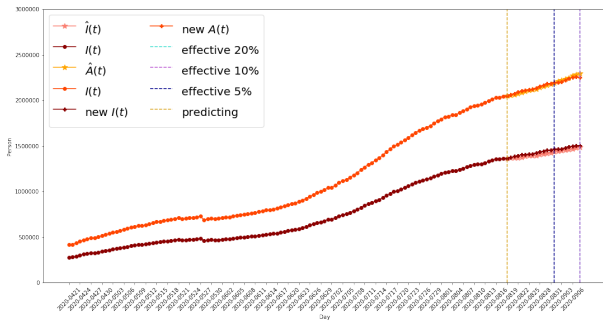


Fig. 9. I, A in US. Date: Apr. 21 ~ Sep. 8. ($\beta, \gamma_1, \gamma_2, \eta$ are respectively 4, 20, 11, 7.)

2) *Fitting the epidemic in Brazil:* For Brazil, we also use 100 data to train model(Phase I in FIG. 10a) and 20 validation data(Phase II in FIG. 10a) to get the effective intervals, 1 day in 5 % relative error(Phase III in FIG. 10a) , 10 days in 10 % relative error(Phase IV in FIG. 10a) and 14 days in 20 % relative error(Phase V in FIG. 10a). Then, we expand our training data to 120 data(Phase I in FIG. 10b) and predict 20 days(Phase II in FIG. 10b). We apply the effective intervals to the forecast: 1 days(Phase III in FIG. 10b), 10 days(Phase IV in FIG. 10b) and 14 days(Phase V in FIG. 10b) in the end.

In FIG. 10a.: Phase I: May. 11 ~ Aug. 19; Phase II: Aug. 19 ~ Sep. 8; Phase III: Aug. 19 ~ Aug. 20; Phase IV: Aug. 19 ~ Aug. 29; Phase V: Aug. 19 ~ Sep. 2.

In FIG. 10b.: Phase I: May. 11 ~ Sep. 8; Phase II: Sep. 8 ~ Sep. 28; Phase III: Sep. 8 ~ Sep. 9; Phase IV: Sep. 8 ~ Sep. 18; Phase V: Sep. 8 ~ Sep. 22.

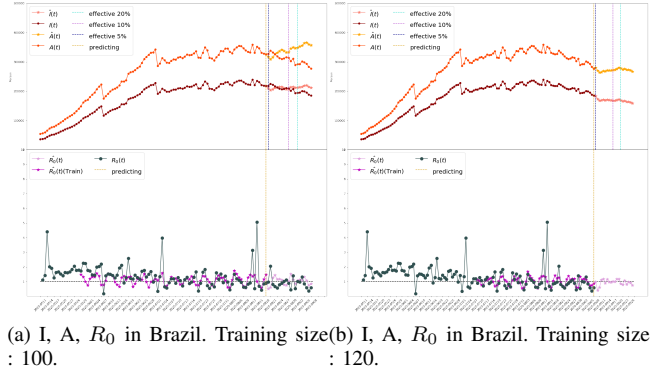


Fig. 10. SIARD Brazil.

FIG.IV-B2 is the comparison of the forecast with real Covid-19 data from Aug.20 to Sep.8 in Brazil.

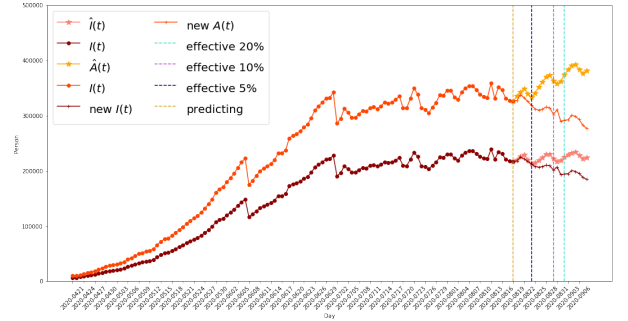
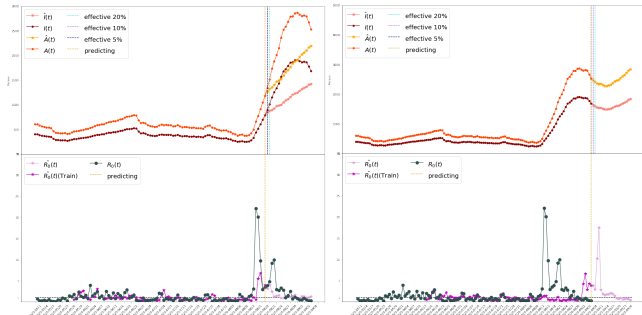


Fig. 11. I, A in Brazil. Date: Apr. 21 ~ Sep. 8. ($\beta, \gamma_1, \gamma_2, \eta$ are respectively 20, 19, 4, 13.)

3) *Fitting the epidemic in South Korea:* Firstly, we take 100 data of South Korea to train the model(Phase I in FIG. 12a) and 20 validation data(Phase II in FIG. 12a) to conduct the effective intervals, 1 day in 10 % relative error(Phase III in FIG. 12a) and 2 days in 20 % relative error(Phase IV in FIG. 12a). Secondly, we expand our training data to 120 data(Phase I in FIG. 12a) and make the forecast for 20 days(Phase II in FIG. 12b). Finally, we implement the effective intervals on the prediction: 1 days(Phase III in FIG. 12b) and 2 days(Phase IV in FIG. 12b).

In FIG. 12a.: Phase I: May. 11 ~ Aug. 19; Phase II: Aug. 19 ~ Sep. 8; Phase III: Aug. 19 ~ Aug. 20; Phase IV: Aug. 19 ~ Aug. 21.

In FIG. 12b.: Phase I: May. 11 ~ Sep. 8; Phase II: Sep. 8 ~ Sep. 28; Phase III: Sep. 28 ~ Sep. 29; Phase IV: Sep. 28 ~ Sep. 30.



(a) I, A, R_0 in Korea. Training size : 100. (b) I, A, R_0 in Korea. Training size : 120.

Fig. 12. SIARD Korea.

The comparison of the forecast with real Covid-19 data from Aug.20 to Sep.8 in South Korea is in FIG.IV-B3.

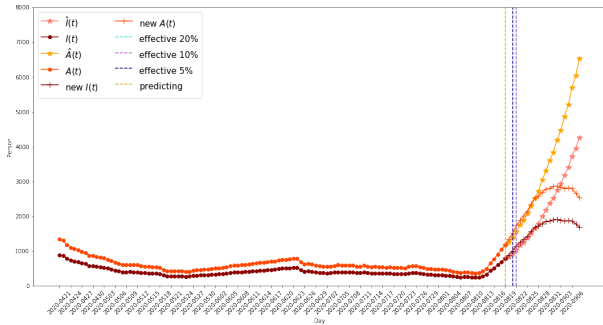
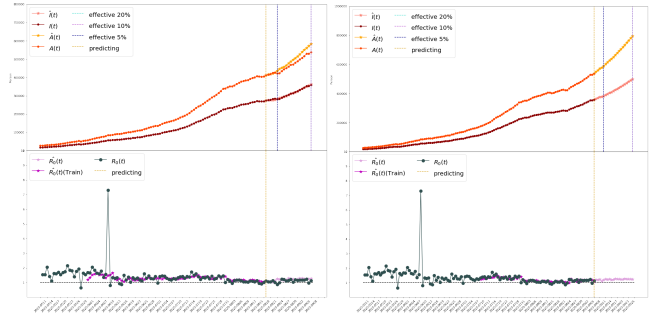


Fig. 13. I, A in Korea. Date: Apr. 21 ~ Sep. 8. ($\beta, \gamma_1, \gamma_2, \eta$ are respectively 10, 13, 13, 6.)

4) *Fitting the epidemic in India:* In India, 100 data are adopted to train model(Phase I in FIG. 14a) and 20 validation data (Phase II in FIG. 14a) Then we get the effective intervals: 5 days in 5 % relative error(Phase III in FIG. 14a) and 20 days in 10 % relative error(Phase IV in FIG. 14a). Furthermore, we expand our training data to 120 data(Phase I in FIG. 14b) and predict for 20 days(Phase II in FIG. 14b). Finally, We apply the effective intervals to the forecast: 5 days(Phase III in FIG. 14b) and 20 days(Phase IV in FIG. 14b) in the end.

In FIG. 14a: Phase I: May. 11 ~ Aug. 19; Phase II: Aug. 19 ~ Sep. 8; Phase III: Aug. 19 ~ Aug. 24; Phase IV: Aug. 19 ~ Sep. 8.

In FIG. 14b.: Phase I: May. 11 ~ Sep. 8; Phase II: Sep. 8 ~ Sep. 28; Phase III: Sep. 8 ~ Sep. 13; Phase IV: Sep. 8 ~ Sep. 28.



(a) I, A, R_0 in India. Training size : 100. (b) I, A, R_0 in India. Training size : 120.

Fig. 14. SIARD India.

FIG.IV-B4 is the comparison of the forecast with real Covid-19 data from Aug.20 to Sep.8 in India.

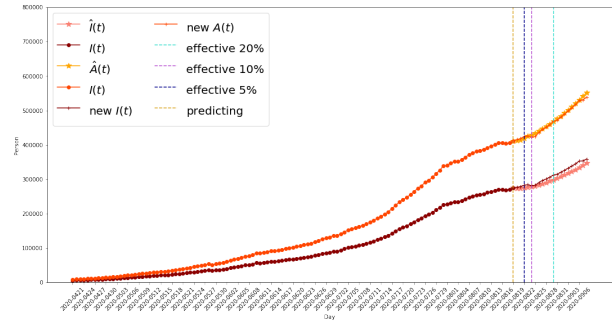
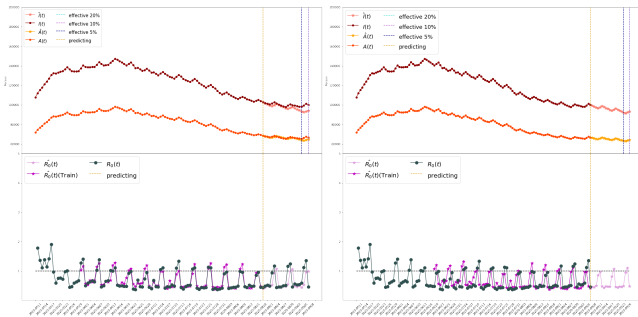


Fig. 15. I, A in India. Date: Apr. 21 ~ Sep. 8. ($\beta, \gamma_1, \gamma_2, \eta$ are respectively 4, 3, 3, 18.)

5) *Fitting the epidemic in Russia:* In the beginning, we adopt 100 data of Russia to train model(Phase I in FIG. 16a) and 20 validation data(Phase II in FIG. 16a). We further obtain the effective intervals for 17 days in 5 % relative error(Phase III in FIG. 16a) and 20 days in 10 % relative error(Phase IV in FIG. 16a). Next, we expand our training data to 120 data(Phase I in FIG. 16b) and predict for 20 days(Phase II in FIG. 16b). Finally, we implement the effective intervals on the prediction in 17 days(Phase III in FIG. 16b) and 20 days(Phase IV in FIG. 16b).

In FIG. 16a.: Phase I: May. 11 ~ Aug. 19; Phase II: Aug. 19 ~ Sep. 8; Phase III: Aug. 19 ~ Sep. 5; Phase IV: Aug. 19 ~ Sep. 8.

In FIG. 16b.: Phase I: May. 11 ~ Sep. 8; Phase II: Sep. 8 ~ Sep. 28; Phase III: Sep. 8 ~ Sep. 25; Phase IV: Sep. 8 ~ Sep. 28.



(a) I, A, R_0 in RUSSIA. Training size : 100. (b) I, A, R_0 in RUSSIA. Training size : 120.

Fig. 16. SIARD Russia.

Comparison of the forecast with real Covid-19 data from Aug.20 to Sep.8 in Russia: FIG.IV-B5.

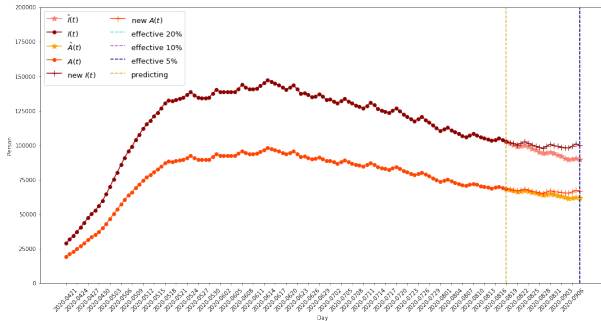
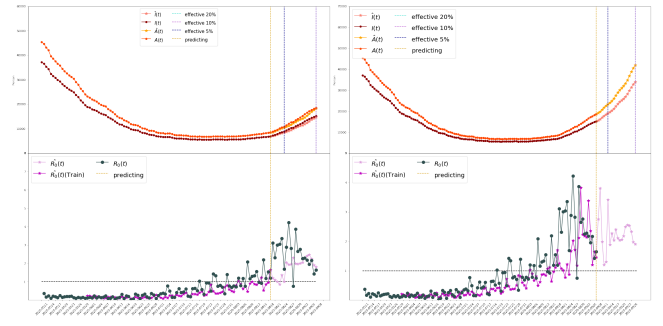


Fig. 17. I, A in Russia. Date: Apr. 21 ~ Sep. 8. ($\beta, \gamma_1, \gamma_2, \eta$ are respectively 13, 15, 15, 7.)

6) *Fitting the epidemic in Italy:* In Italy, 100 data are taken to train the model(Phase I in FIG. 18a) and 20 validation data(Phase II in FIG. 18a) for getting the effective intervals: 6 days in 5 % relative error(Phase III in FIG. 18a) and 20 days in 10 % relative error(Phase IV in FIG. 18a). Then, we expand our training data to 120 data(Phase I in FIG. 18b) and predict for 20 days(Phase II in FIG. 18b). We apply the effective intervals to the forecast in 6 days(Phase III in FIG. 18b) and 20 days(Phase IV in FIG. 18b) in the end.

In FIG. 18a.: Phase I: May. 11 ~ Aug. 19; Phase II: Aug. 19 ~ Sep. 8; Phase III: Aug. 19 ~ Aug. 25; Phase IV: Aug. 19 ~ Sep. 8.

In FIG. 18b.: Phase I: May. 11 ~ Sep. 8; Phase II: Sep. 8 ~ Sep. 28; Phase III: Sep. 8 ~ Sep. 14; Phase IV: Sep. 8 ~ Sep. 28.



(a) I, A, R_0 in ITALY. Training size : 100. (b) I, A, R_0 in ITALY. Training size : 120.

Fig. 18. SIARD Italy.

FIG.IV-B6 is the comparison of the forecast with real Covid-19 data from Aug.20 to Sep.8 in Italy.

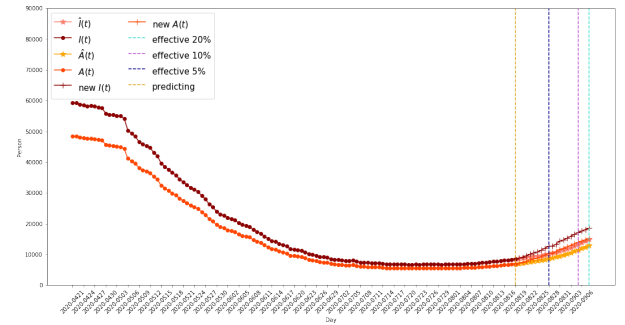


Fig. 19. I, A in Italy. Date: Apr. 21 ~ Sep. 8. ($\beta, \gamma_1, \gamma_2, \eta$ are respectively 19, 19, 19, 2.)

C. Comparison and Analysis of Forecasting Effects

Our model finds the proportion of people with symptoms α in six countries. For example, in Table 1, the proportion of symptomatic infections in Italy is about 55 %, which means that the proportion of asymptomatic infections in the country is about 45 %. This is in line with the 43.2 % of asymptomatic infections obtained by the authors of [2] at V'ò, Italy. It proves that our model does have the ability to judge the proportion of asymptomatic infections.

By above figures in US, Brazil, South Korea, India, Russia, and Italy, it is obvious that the trend of symptom and asymptomatic are in relation with R_0 . When R_0 increase, I and A also increase, same as decrease. In other words, R_0 can be viewed as an important target of the break or not of the COVID-19.

According to the result of our prediction, the amount of prediction days which more precisely depends on the origin data. For example, since the data of Russia change periodically or decrease on the whole, we can try to find out the appropriate order for the Country and predict more days. In contrast, like South Korea, the data in South Korea changes unsteadily and exists an extreme value, so we can not predict more days.

In US, we have the data of quarantine, so we can apply SQIARD model to predict data in future. Since we add extra parameters into model, especially the speed rate from quarantine to symptom or asymptomatic, we can predict the data more precisely than SIARD. For instance, we use SIARD model to predict, the effective interval has 8 days(FIG. 8a.). However, when we use SQIARD model to predict, we can predict about 15 days(FIG. 6a.), so the way of SQIARD model to perform is better than SIARD model during this period.

REFERENCES

- [1] S. Flaxman, et al., Estimating the effects of non-pharmaceutical interventions on COVID-19 in Europe, *Nature* (2020) <https://doi.org/10.1038/s41586-020-2405-7>.
- [2] E. Lavezzo, et al., Suppression of a SARS-CoV-2 outbreak in the Italian municipality of Vo', *Nature* (2020) <https://doi.org/10.1038/s41586-020-2488-1>.
- [3] Avila-Ponce de León, Ugo; Pérez, Ángel G. C.; Avila-Vales, Eric; An SEIARD epidemic model for COVID-19 in Mexico: Mathematical analysis and state-level forecast. *Chaos Solitons Fractals* 140 (2020), 1
- [4] D.F. Gudbjartsson, et al., Spread of SARS-CoV-2 in the Icelandic population, *N. Engl. J. Med.* (2020) <http://dx.doi.org/10.1056/NEJMoa2006100>.
- [5] Mizumoto Kenji, Kagaya Katsushi, Zarebski Alexander, Chowell Gerardo. Estimating the asymptomatic proportion of coronavirus disease 2019 (COVID-19) cases on board the Diamond Princess cruise ship, Yokohama, Japan, 2020. *Euro Surveill.* 2020;25(10):pii=2000180. <https://doi.org/10.2807/1560-7917.ES.2020.25.10.2000180>
- [6] W.O. Kermack, e A.G. McKendrick, Contributions to the mathematical theory of epidemics, *Proc. R. Soc. Lond. Ser. A Math. Phys. Eng. Sci.* 138 (1932) 55–83; *Proc. R. Soc. Lond.* a 141 (1933) 94–122.
- [7] Sze-Bi Hsu, Ying-Hen Hsieh. On the Role of Asymptomatic Infection in Transmission Dynamics of Infectious Diseases. *Bulletin of Mathematical Biology*, (2008) 70: 134–155
- [8] Sze-Bi Hsu, Ying-Hen Hsieh. Modeling International Measures and Severity-Dependent Public Response During Severe Acute Respiratory Syndrome Outbreak. *SIAM J. APPL. MATH.*, (2006) Vol. 66, No. 2, pp. 627–647
- [9] P. Samui, J. Mondal and S. Khajanchi, A mathematical model for COVID-19 transmission dynamics with a case study of India, *Chaos, Solitons and Fractals* 140 (2020) 110173 <https://doi.org/10.1016/j.chaos.2020.110173>
- [10] Yi-Cheng Chen, Ping-En Luy, Graduate Student Member, IEEE, Cheng-Shang Chang, Fellow, IEEE, and Tzu-Hsuan Liux. A Time-dependent SIR model for COVID-19 with Undetectable Infected Persons. *IEEE* (2020)
- [11] G. Bastin. Lectures on Mathematical Modelling of Biological Systems (2018)
- [12] P. van den Driessche, James Watmough. Reproduction numbers and sub-threshold endemic equilibria for compartmental models of disease transmission. *Mathematical Biosciences*, (2002) 180 29–48
- [13] COVID-19 Data: <https://data.humdata.org/dataset/novel-coronavirus-2019-ncov-cases>
- [14] COVID-19 Data for US: <https://covidtracking.com/>
- [15] WHO: <https://www.who.int/emergencies/diseases/novel-coronavirus-2019>